Spurious Parametric Oscillations in IMPATT Diode Circuits

By W. E. SCHROEDER

(Manuscript received December 26, 1973)

This paper describes a quantitative experimental confirmation of a recent theory for large-signal parametric instabilities in IMPATT diode circuits. The relevant parts of the theory are presented in a concise form. A graphical technique is given that is useful for analyzing circuit stability. A sufficient (though not necessary) condition for well-behaved circuits is also studied, and several diagrams are presented that may prove useful to circuit designers.

I. INTRODUCTION

Spurious oscillations are frequently observed in strongly driven IMPATT amplifiers and oscillators. Spurious oscillation is a generic term that means, in the case of an amplifier, that there is a signal frequency in the output not present in the input and, in the case of an oscillator, that there is a signal present in addition to the main desired oscillation. In IMPATT diode circuits, the type of spurious oscillation most frequently observed fits into one of two categories: (i) a parametric-pair-type instability in which there are two spurious signals whose frequencies sum to equal that of the strong signal or (ii) a subharmonic instability in which one spurious signal occurs at one-half the frequency

of the strong signal. It is evident that the second category is a special case of the first, and may be considered a degenerate parametric oscillation.

In the course of experiments on IMPATT amplifiers and locked oscillators, both degenerate and nondegenerate parametric instabilities have been encountered. Accompanying the onset of spurious oscillation, it has been noted that there is often a saturation of rf output power, a degradation of the amplifier's noise performance, and/or a shift in the center frequency of the locking band. Although the spurious signals themselves are generally undesirable, the adverse effects upon amplifier performance at the design frequency are even more serious. Therefore, it is important to understand the nature of the spurious oscillations and to determine what must be done to the amplifier design to eliminate them.

In a recent paper, M. E. Hines[1] presented a theory for parametric interactions in IMPATT diodes, which is based on the nonlinear inductive behavior of the avalanche process. He has given an expression for the stability of the IMPATT diode-microwave circuit system.

This paper describes experiments conducted to characterize the diode and circuit conditions at the onset of spurious oscillation, for both degenerate and nondegenerate cases, and to compare the results with Hines' theory. Good quantitative agreement was found between our experimental observations and the predictions of a simplified form of Hines' stability expression. Thus, it appears that Hines' theory forms a sound basis for designing circuits to suppress parametric-type spurious oscillations.

In another section of this paper, we discuss a procedure for determining a region of impedance such that, if the circuit impedance (as seen by the diode) lies within this region, the diode-circuit system is stable against parametric oscillations for all drive levels. It appears that this stable impedance region is physically obtainable, and further that it is compatible with the impedance requirements discussed by Brackett[2] with regard to suppressing bias-circuit oscillations that are due to a phenomenon different from the one considered by Hines.

II. REVIEW OF HINES' THEORY

In this section a brief recapitulation is given of the aspects of Hines' theory that are pertinent to the stability of parametric interactions in IMPATT diodes.

Hines uses the Read[3] model of an IMPATT diode to derive an equivalent circuit for parametric interaction of the form given in Fig. 1.
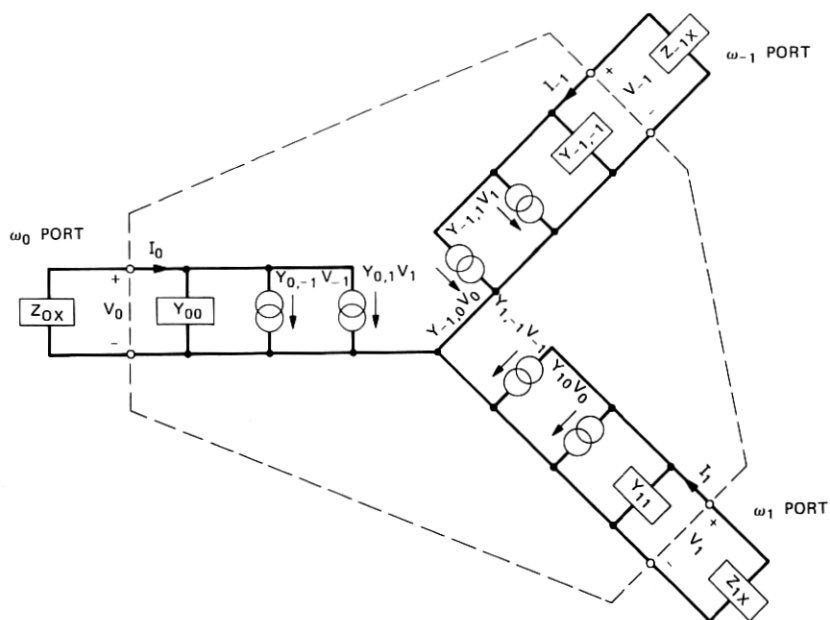
Fig. 1—Equivalent circuit for parametric interaction.

The equivalent circuit is applicable to small-signal parametric interactions when the diode is in some large-signal "pumped" state. The pump frequency ω_p is defined as the fundamental frequency of the large-amplitude pump wave that is present at the diode. The pump wave arises from the impressed signal in the case of an amplifier or from the circuit-controlled oscillation in the case of an oscillator. The parametrically related frequencies ω_m are defined as follows:

$$\omega_0 \triangleq \text{the lowest perturbing frequency (\textit{not} the}$$
$$\text{main oscillation frequency)} \tag{1}$$

and

$$\omega_1 \triangleq \omega_p + \omega_0, \tag{2}$$

$$\omega_{-1} \triangleq \omega_p - \omega_0^*, \tag{3}$$

where the asterisk denotes complex conjugate.

From Fig. 1, it is evident that the current I_0 at ω_0 consists of three components: current due to the self-admittance at ω_0 and current induced by the presence of parametrically related voltages at the upper

and lower sidebands, ω_1 and ω_{-1}, respectively. Contributions to I_0 from the higher-order parametric signals at the frequencies $n \cdot \omega_p \pm \omega_0$ for $n \geq 2$ have been neglected. The equivalent circuit for the sidebands is similar. The impedance Z_{mx} is the external impedance presented to the diode wafer at the frequency ω_m. The diode package and mount parasitic impedances are included in Z_{mx}. The pump frequency of the diode does not appear directly in the equivalent circuit, but the pump state is introduced through the admittances $Y_{m,n}$.

From this equivalent circuit Hines derived the following characteristic equation, which governs the stability of the diode-circuit system:

$$D \triangleq 1 - M_1 M_{-1} S_0 (S_{-1}^* + S_1) - M_2 M_{-2} S_1 S_{-1}^*$$
$$+ (M_1^2 M_{-2} + M_{-1}^2 M_2) S_0 S_1 S_{-1}^* \qquad \text{(Hines eq. 23)}$$
$$= 0. \qquad (4)$$

The complex quantity M_n is defined as the avalanche particle current at the nth pump harmonic divided by the dc current. Note that here the subscript n signifies the frequency $n \cdot \omega_p$, whereas the subscripts of the S quantities refer to the parametric frequencies ω_m. It is also important to note that

$$M_n = M_{-n}^* \qquad (5)$$

and

$$|M_n| \leq 1. \qquad (6)$$

Generally, $|M_n|$ increases monotonically with the pump level and approaches unity as the avalanche current approaches a sharp, narrow pulse.

The complex quantities S_m may be thought of as stability factors. They are defined as:

$$S_m = S(\omega_m) = 1 + \left(\frac{\omega_m^2}{\omega_a^2 - \omega_m^2} \right) \frac{Z_x(\omega_m) + 1/j\omega_m C_T}{Z_x(\omega_m) + Z_d(\omega_m)} , \qquad (7)$$

where

ω_a = avalanche resonance frequency of the diode,
C_T = total "cold" capacitance of the diode, i.e., that of the entire depleted region,

and

$$Z_d(\omega) = \frac{\bar{x}_d - \bar{x}_d (\sin \theta_d / \theta_d) - \omega^2/\omega_a^2 + j\bar{x}_d [(1 - \cos \theta_d)/\theta_d]}{j\omega C_T (1 - \omega^2/\omega_a^2)} , \qquad (8)$$

where

$$\bar{x}_d = \text{ratio of drift length to total length of the diode}$$

and

$$\theta_d = \omega \tau_d = \text{transit angle of the drift region.}$$

The quantity Z_d is the small-signal Read-model admittance previously derived by Gilden and Hines.[4]

The stability of the diode-circuit system may be studied by examining the roots of eq. (4) for complex frequency. It is apparent that the effect of the large-signal pump state upon stability is completely described by the two factors M_1 and M_2, since the stability factors S depend only upon the *small-signal* diode impedance and the circuit impedance. This separation of pump level and circuit impedance effects is a very useful aspect of Hines' approach. It avoids entangling the stability discussion with the details of the large-signal nonlinear diode behavior. If, for a given circuit and diode, the stability factors are such that there are no unstable roots for $0 < |M_1| < 1$ and $0 < |M_2| < 1$, then the system is stable for any pump level.

Under certain conditions, simplified forms of the characteristic equation are valid and useful. For instance, if $|M_2| \ll |M_1|$, which corresponds to intermediate pump levels, then eq. (4) becomes

$$1 - |M_1|^2 S_0 (S_{-1}^* + S_1) \cong 0. \tag{9}$$

Alternatively, if $|S_1| \ll |S_0|$ and $|S_{-1}|$ then eq. (4) simplifies to

$$1 - |M_1|^2 S_0 S_{-1}^* \cong 0. \tag{10}$$

The simplified criterion given by eq. (10) is the one suggested by Hines for the degenerate case, but it is applicable to the nondegenerate case as well. We have found good agreement between our experimental observations and eq. (10), as is discussed in the next section.

The approximation which leads to eq. (10) may be justified by examination of the definition of S: For $\omega \ll \omega_a$, the term $\omega^2/(\omega_a^2 - \omega^2)$ is much smaller than 1 and $S(\omega)$ approaches unity. For ω in the vicinity of ω_a, $Z_d(\omega)$ is quite different from $1/j\omega C_T$ and of course $\omega^2/(\omega_a^2 - \omega^2)$ is large: therefore, $S(\omega)$ is not in general negligible. However, there is no pole for $S(\omega = \omega_a)$, since the pole in Z_d cancels that of $\omega^2/(\omega_a^2 - \omega^2)$. Since it is usually desirable to pump the diode where the negative conductance is large, $\omega_p^2 \geq 2\omega_a^2$ is generally true. Therefore, for $\omega > \omega_p$

$$\frac{\omega^2}{\omega_a^2 - \omega^2} \rightarrow -1$$

and also

$$Z_d \rightarrow \frac{1}{j\omega C_T},$$

and, therefore, $S(\omega)$ tends ultimately to zero. Therefore, eq. (10) seems to be a reasonable approximation, especially for $\omega_0 \approx \omega_p/2$.

In order to study stability, the characteristic function D is considered a function of complex frequency $p = \sigma + j\omega$. Instability occurs if the zeros of D lie in the right half of the p-plane. In the case of spurious oscillation in IMPATT diodes, it is an experimental fact that for sufficiently small M_1 there is no instability; thus, the zeros of D (and the poles of $S_0S_{-1}^*$) must lie in the left half of the p-plane for small M_1. As M_1 is increased to its maximum value of 1, the roots of D may or may not cross into the right half of the p-plane. Assuming that the roots of D vary continuously with M_1, then any crossing into the right half of the plane implies that there is first an intersection of the root locus with the imaginary axis for some value of M_1. The frequency for which the zero of D lies on the $p = j\omega$ axis may be designated as $\bar{\omega}$ and the corresponding value of M_1 as $\bar{M}_1$. For $M_1 = \bar{M}_1$, the system is said to be marginally stable or at the threshold of spurious oscillation, where the spurious frequency is $\bar{\omega}$.

Thus, in order to determine approximately if a given diode and circuit are unstable for a physically attainable pump condition, it is only necessary to evaluate $D \cong 1 - |M_1|^2 S_0 S_{-1}^*$ for *real* ω (actually, just for $0 < \omega_0 < \omega_p/2$) and determine if there are any zeros for $0 < |M_1| < 1$. If not, then the system is stable for any pump level. If there are zeros, then the zero with the smallest value of $|M_1|$ corresponds to the first spurious oscillation which we would expect to observe upon increasing the pump level monotonically from zero. In this case, we may predict the drive level and the frequency for the onset of spurious oscillation.

It is evident that zeros of D correspond to real values of $S_0S_{-1}^*$. Thus, we may plot $S_0S_{-1}^*$ and note the frequencies where the locus intercepts the real axis. The basic construction for one value of ω_0 is indicated schematically in Fig. 2. There is at least one real axis intercept since, for $\omega_0 = \omega_p/2$, $S_0 = S_{-1}$. This is not necessarily an instability, since $|S(\omega_p/2)|$ may be less than 1. Since the phase condition for instability is always satisfied at the subharmonic, this suggests that the half-pump frequency oscillation may be a more likely form of spurious output, which appears to agree with the experience of many workers.
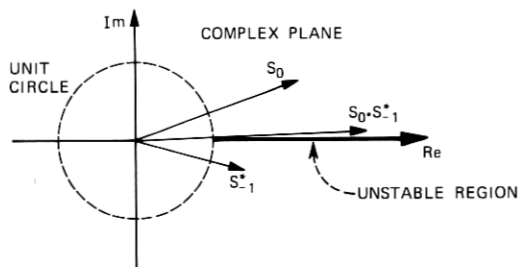
Fig. 2—Schematic diagram of the simplified stability criterion.

It is interesting to note that eq. (10) has the same form as the expression for stability of a single-loop feedback control system, $1 + kG(\omega)H(\omega) = 0$, where $G(\omega)$ is the forward gain and $kH(\omega)$ is the gain of the feedback loop. Thus the modulation index M_1 is analogous to the gain of a feedback loop. This suggests that some concepts of classical control theory may be useful in the present problem.

III. COMPARISON OF OBSERVED SPURIOUS OSCILLATIONS WITH THE STABILITY CRITERION

In this section, an experiment is discussed in which the onset of spurious oscillation was observed and characterized for three diode-circuit cases. Both degenerate and nondegenerate parametric-type oscillations were obtained. The predictions of the simplified stability criterion of eq. (10) are found to be in good agreement with the experiments.

The basic idea of the experiment is to place the diode-circuit system in a state that corresponds to the onset of spurious oscillation. Then that threshold state is characterized by measuring $Z_x(\omega)$, $Z_d(\omega)$, the pump level and the spurious frequencies. The results may be compared with the predictions of the stability theory.

There are several ways in which the diode-circuit system may be placed in the threshold state. One way is to operate the circuit as an amplifier; with the diode bias current and the circuit tuning held constant, the input signal level may be increased until spurious output begins. Another way is to operate the circuit as an oscillator where the diode current is fixed and the tuning is varied in such a way as to increase the oscillation strength until spurious oscillation begins. Still another way is to operate the circuit as a fixed-tuned oscillator and increase the dc bias current, thereby increasing the oscillation strength

until instability occurs. We have experimented with each method and found that the nature of the spurious oscillations appears to be the same in each case. For reasons of experimental convenience, the second method has been adopted, with the results described here.

The experimental setup is shown in the schematic diagram of Fig. 3. The circuit is a circulator-coupled, locked-oscillator-type amplifier designed to operate at 11 GHz with a single 2-watt GaAs IMPATT diode. The oscillation frequency is primarily controlled by the capacitive disc, and the tuning screws are used for impedance trimming. The experimental procedure is to position the screws so that the diode may be biased at full operating current without oscillation of any kind. Next, the tuning screws are adjusted so that oscillation is initiated at about 11 GHz, the pump signal frequency. Then the screws are adjusted to further load the diode so that it delivers progressively more pump power until spurious oscillation begins. At the onset of spurious output, the pump output power and frequency are recorded along with the frequency of the spurious signal or signals, and the circuit impedance is then measured.

Several cases of spurious oscillation were investigated using this procedure. The data characterizing the situation at the onset of instability are summarized in Table I. A more complete discussion of the cases is given below.

Case 1. The diode was biased to $I_{dc} = 300$ mA. In the initial position of the tuning screws, there was no oscillation of any kind. As the screw penetration was increased, the diode began to oscillate near 11 GHz and the output power increased monotonically with screw penetration. There was a slight continuous shift in f_p of about 200 MHz, as the output power was increased up to and somewhat beyond the threshold of spurious output. The output pump power is defined as the power available (at f_p) at the output port of the circulator in Fig. 3.

When the tuning was adjusted past the threshold point, both the subharmonic signal and the pump grew stronger. No additional spurious signals were observed.

At the threshold condition, the output spectrum was carefully searched from 10 MHz to 40 GHz with the following results. No spurious signals were found other than the weak subharmonic signal. In particular, no signal could be detected at the upper sideband frequency, $\omega_1 = 1.5\omega_p$. This provides support for the idea that S_1 may often be negligible, which is the approximation used to reduce eq. (4) to eq. (10). A relatively weak signal was detected at $f = 2f_p$, but not at the third harmonic of the pump. Harmonics of the pump signal are
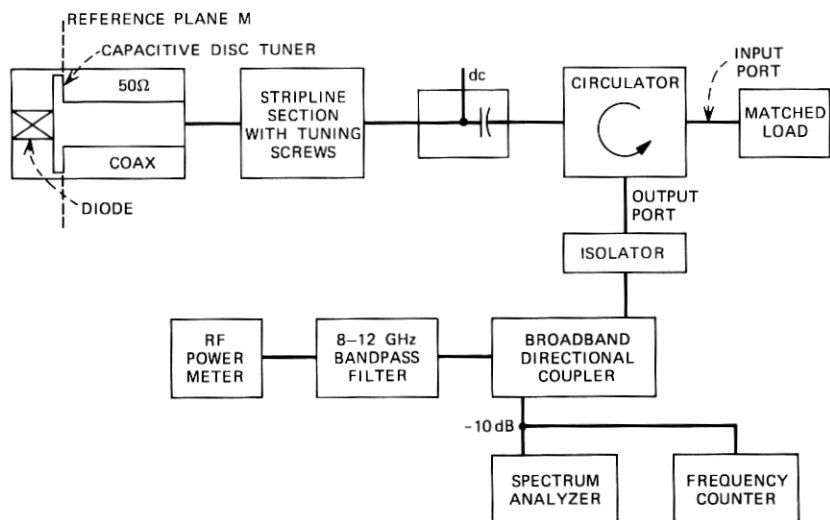
Fig. 3—Schematic diagram of the experimental setup.

not considered to be spurious signals, since in any nonlinear device harmonic components are expected when strongly driven. Note that the second harmonic factor M_2 does not affect the spurious oscillation condition when S_1 is small.

The diode used for this case, diode 15, is a one-sided, uniformly doped, Schottky-barrier, GaAs diode.

Case 2. The circuit used in this case is the same as in case 1; the only difference is in the positions of the tuning screws. The diode used here, diode 2, is similar in type to diode 15. The major difference between

Table I — Summary of experimental data at the threshold of parametric instability

	Case 1	Case 2	Case 3
Diode used	#15	#2	#15
Pump frequency, GHz	11.0988	11.1135	10.94
Pump power, dBm	25.5	28.4	27.0
Spurious type and frequency, GHz	Subharmonic $f_0 = f_{-1}$ $= 5.5494$	Subharmonic $f_0 = f_{-1}$ $= 5.5567$	Two-frequency $f_0 = 4.61$; $f_{-1} = 6.33$
I_{dc}, mA	300	300	300
V_{dc}, V	59.7	67.2	59.5

the diodes is that diode 2 has a smaller area (by a factor of 0.73) and, thus, a higher impedance level than diode 15.

The spurious threshold for this case corresponds to nearly 3 dB more output power than for case 1. Otherwise, the two cases are very similar. The pump frequency is essentially the same, the spurious type is subharmonic, and no other spurious signals were observed at the threshold.

Case 3. In this case, diode 15 is used again. The circuit is modified from that shown in Fig. 3 by the inclusion of a shunt line which is $\lambda/4$ long at about 5.5 GHz. The line is connected to the capacitive disc through a small resistor and is terminated with an open circuit at the distant end. The idea is to alter Z_x at the subharmonic without affecting Z_x at the pump frequency.

It is apparent that the desired effect was obtained, in that the diode may now be driven to a higher output level than in case 1 without obtaining spurious tones. Further, when an instability develops, it turns out to be a parametric pair rather than the subharmonic described in case 1. Other than f_0 and f_{-1}, which are given in Table I, no other spurious signals were observed.

It was possible to vary the tuning screws to keep the diode-circuit system at the threshold condition while reducing f_p by about 80 MHz from the value given in the table. As this was done, both f_0 and f_{-1} decreased by approximately 40 MHz each. Thus, apparently neither spurious signal is frequency-dominant in this case.

3.1 Calculation of theoretical spurious threshold

To apply the simplified stability criterion of eq. (10) to predict the spurious threshold for the experimental cases, the diode impedance $Z_d(\omega)$ and the external circuit impedance $Z_x(\omega)$ must be determined. The small-signal impedance of the diodes in question was directly measured for $I_{dc} = 300$ mA by a method that has been described in detail elsewhere.[5] Since Hines' theory is cast in terms of the Read-diode model, what are actually needed are the values of the parameters in the Read-model expression for Z_d [see eq. (8)], which best fit the measured impedance of the real diode. A comparison of the measured small-signal admittance data and the equivalent Read admittance expression is given for both diodes in Figs. 4a and 4b. It is apparent that the agreement is not exact, but it is good enough for our purpose. The corresponding diode parameter values are given in Table II.

The other impedance required is Z_x, the external impedance, which is defined as the impedance seen by the diode wafer. It, therefore,
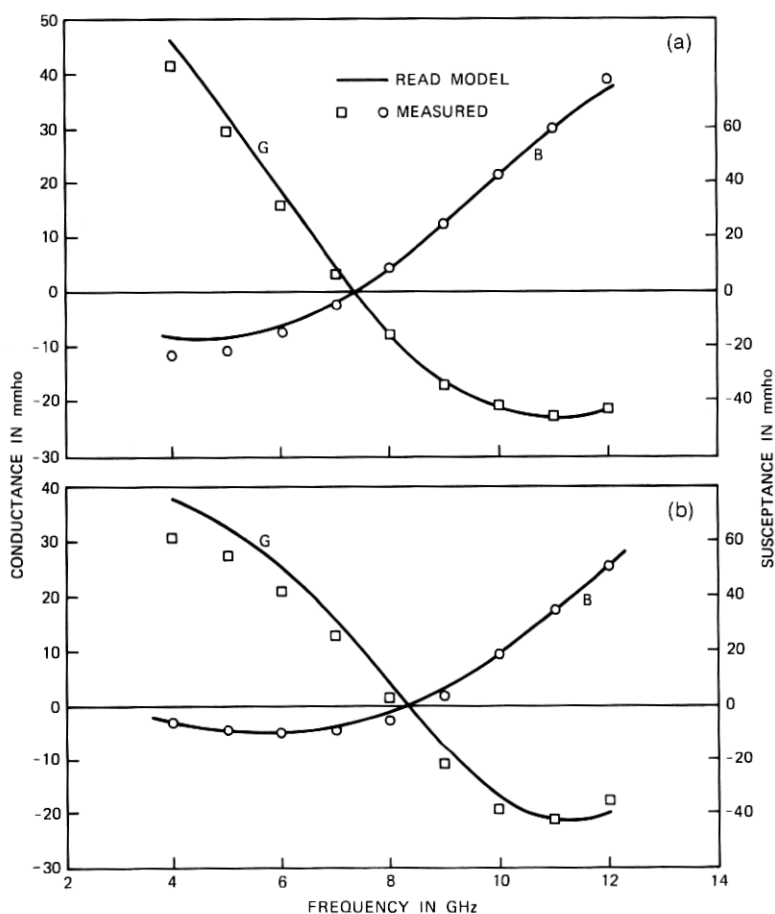
Fig. 4—Comparison of measured small-signal wafer admittance with the Read-model equivalent (I_{dc} = 300 mA). (a) Diode 15. (b) Diode 2.

Table II — Parameter values for the Read-model equivalent of diodes 2 and 15

Parameter	Diode 2	Diode 15
C_T^*, pF	0.86	1.176
f_a, GHz	8.3	7.35
τ_d, ps	44.8	41.5
$\bar{x}_d$, dimensionless	0.83	0.83

* These values of C_T are appropriate for the operating temperature.

must include the parasitic elements contributed by the diode package and mount. The equivalent circuit for this is shown in Fig. 5. The quantity Z_m is the impedance at the reference plane M (see Fig. 3) looking toward the circulator. The element values given in Fig. 5 were determined by making a series of impedance measurements at the plane M looking toward the wafer and replacing the packaged diode with each of several standard impedances. Comparison of the measured element values with the geometry of the circuit reveals that: (i) L_s is equal to the inductance associated with the lead wire internal to the package, (ii) C_1 is composed partly of the package capacitance and partly of mount capacitance directly in parallel with the conventional C_p, (iii) L_M is due to magnetic energy storage within the annular region between the package and the outer conductor, and (iv) C_2 is due to the fringing and gap capacitance of the disc. Because of differences in internal construction, $L_s = 0.330 \ nH$ for diode 2 and $L_s = 0.278 \ nH$ for diode 15. The parameters C_1, C_2, and L_M are the same for each of the three spurious oscillation cases. The impedance Z_M was measured at 100-MHz intervals using a Hewlett-Packard automatic network analyzer. In each case, the tuning screws were in the position that corresponded to the onset of spurious oscillation.

The resulting Z_x for cases 1 and 3 are shown in Smith chart form in Figs. 6a and 6b. In case 2, Z_x is found to be similar but not identical to case 1; the differences are due to different screw positions and different L_s values. An independent corroboration of the measured Z_x may be obtained by observing that, since the diode oscillated at a known frequency in each case, then $-Z_x(\omega_p)$ must be equal to the large-signal diode impedance. Note that $-Z_x(\omega_p) \neq Z_d(\omega_p)$, since the large-signal impedance is somewhat different from Z_d. Such a comparison was made for case 1 using the theoretical large-signal result computed[6] for a very similar diode structure when operated at the same rf efficiency, and the agreement was found to be quite good.
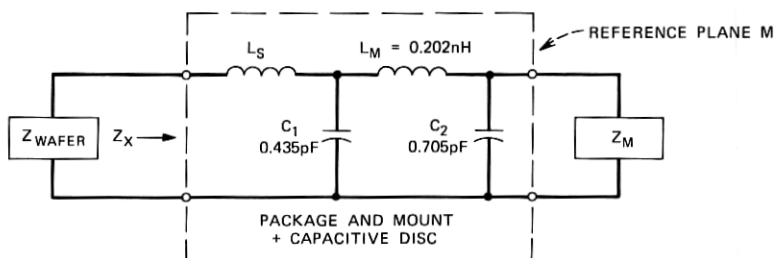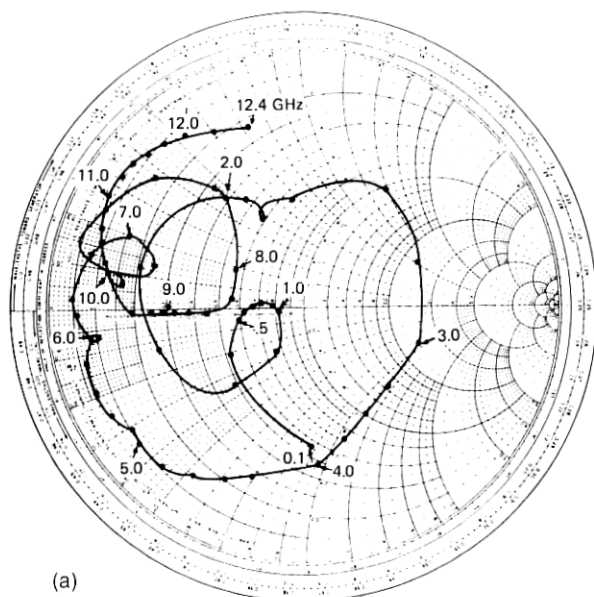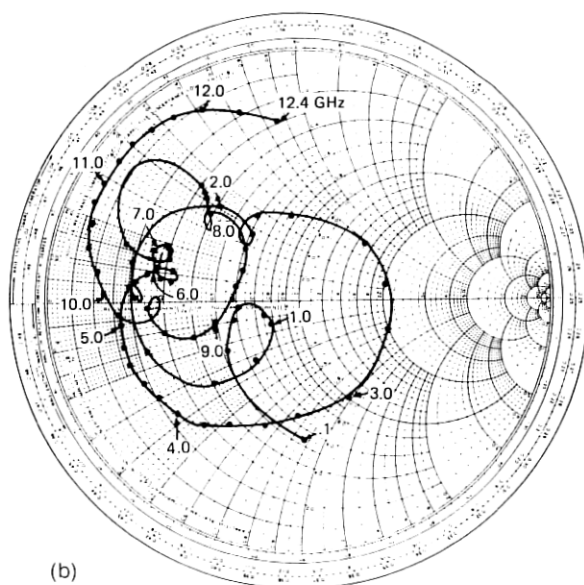

Fig. 5—Equivalent circuit for the diode package and mount.

Fig. 6—External impedance normalized to 50 ohms. (a) Case 1. (b) Case 3.

Using the Z_x and Z_d data, the S-factor has been computed for each case. When the pump frequency is established, the quantity $S_0S_{-1}^*$ may then be evaluated. This dimensionless quantity is plotted in Figs. 7a to 7c for each of the three cases.

In case 1, it is evident that there is only one intercept with the real axis. This occurs at $S_0S_{-1}^* = 2.68$ for $f_0 = 5.55$ GHz, i.e., at the subharmonic frequency. Thus, there is only one potential spurious oscilla-
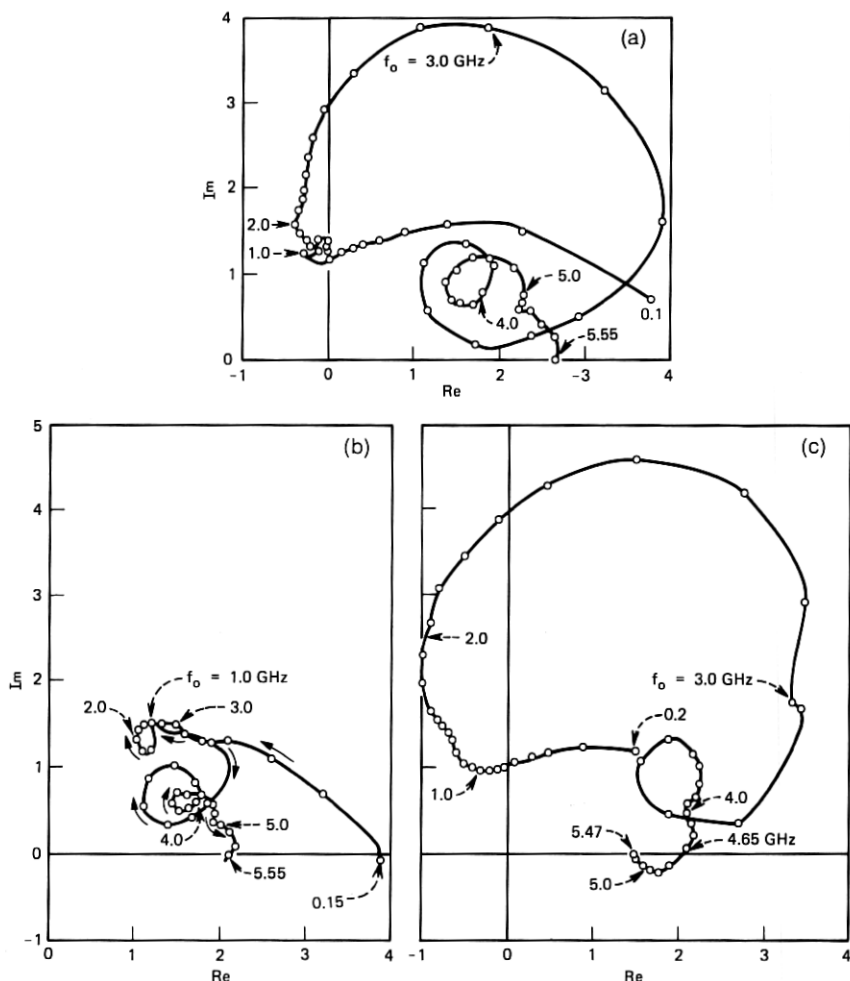

Fig. 7—Stability factor product $S_0S_{-1}^*$ as a function of ω_0. (a) Case 1. (b) Case 2. (c) Case 3.

tion for this case. Since the intercept is larger than one, the subharmonic oscillation is expected to occur for physically attainable pump levels, specifically for $|M_1| \geq (2.68)^{-\frac{1}{2}} = 0.611$. Experimentally, the spurious oscillation observed was indeed of the subharmonic type, and it began at 25.5-dBm pump power.

In case 2, it is seen that if the behavior of $S_0 S_{-1}^*$ at the extreme low frequency limit is neglected for the moment, there is again only one intercept with the real axis. Thus, again the diode is potentially unstable at the subharmonic only, and instability is expected for $|M_1| \geq 0.678$. Experimentally, subharmonic oscillation was observed to begin for pump power equal to 28.4 dBm. This is significantly higher than the threshold pump power for case 1 and is in agreement with the fact that the predicted threshold M_1 level is higher for case 2.

The general appearance of the $S_0 S_{-1}^*$ plot in case 2 is quite different from case 1. This is primarily due to the higher diode impedance level in case 2, since $Z_x(\omega)$ is very similar in both cases. A check of the Z_x data in the vicinity of the subharmonic reveals that they are virtually identical for cases 1 and 2. Thus, the predicted and observed higher degree of stability for diode 2 in the basic amplifier circuit is primarily due to the smaller junction cross-sectional area of diode 2.

Let us now consider the approach of $S_0 S_{-1}^*$ toward the real axis for f_0 less than 200 MHz. This behavior indicates a potential instability for $f_0 \cong 150$ MHz and $f_{-1} \cong 10.96$ GHz, which was not experimentally observed. A likely explanation for this is that, for very small ω_0, the upper and lower sidebands are close to ω_p and, therefore, the quantity S_1 is no longer negligible. That is, the more complete stability criterion is probably required for $\omega_0 \ll \omega_{p/2}$. Also, for very small ω_0 the rectification effect which is neglected in this large-signal model becomes important and may affect the stability.

In case 3, there are two intercepts of the real axis:

$$S_0 S_{-1}^* = \begin{cases} 2.07 \text{ for } f_0 = 4.65; \ f_{-1} = 6.29 \text{ GHz} \\ 1.52 \text{ for } f_0 = 5.46 = f_{-1}. \end{cases}$$

Thus, there are two potentially unstable parametric pairs, and it is expected that the nondegenerate pair would be the instability encountered by increasing the pump level until spurious oscillation begins. The associated threshold pump level is $|M_1| = 0.695$. The observed spurious oscillation was a parametric pair at 4.61 and 6.33 GHz, which is considered to be in quite good agreement with the predicted values. The threshold pump power was 27.0 dBm, which is clearly larger than that required to initiate instability for the same

diode in case 1. The latter fact agrees with the predicted relative stability of the two cases.

Thus, there is good agreement between the instability theoretically predicted, using the simplified stability criterion of eq. (10), and that experimentally observed in all three cases.

IV. THEORETICAL STUDY OF CIRCUIT IMPEDANCE SUFFICIENT FOR UNCONDITIONAL STABILITY

As was discussed in the introduction, spurious oscillation is usually an undesirable phenomenon for a number of reasons. Thus, it is of interest to determine what, if anything, can be done to the diode-circuit system to insure that an instability cannot occur. Applying a stability criterion to this synthesis problem is generally more difficult than analyzing a given situation for stability. However, some useful information can be obtained from the simple stability criterion of eq. (10), which was shown in the previous section to predict spurious oscillation accurately for several experimental cases.

To obtain unconditional stability, it is necessary to have an $S_0 S_{-1}^*$ function that does not intersect the real axis beyond unity for $0 \leq \omega_0 \leq \omega_{p/2}$, as indicated in Fig. 2. It is sufficient for unconditional stability if $S_0 S_{-1}^*$ lies within the unit circle. However, the latter condition is not required for stability except in the special case of the subharmonic. Figures 7a to 7c contain numerous examples of frequencies for which $|S_0 S_{-1}^*|$ is quite large, yet instability did not occur there, because the phase requirement was not satisfied.

Although the requirement that $S_0 S_{-1}^*$ should lie within the unit circle is somewhat restrictive, it has the advantage that one may concentrate on reducing the magnitudes of S_0 and S_{-1} and completely disregard the phase of the stability factors. This simplifies the problem greatly. If the additional requirement is made that S_0 and S_{-1} should each lie within the unit circle, a further simplification results. It is then no longer necessary to consider the pump frequency explicitly since, no matter what the value of ω_p is, $S_0 S_{-1}^*$ must lie within the unit disc. Therefore, most of this section is concerned with the conditions that must be satisfied to give $|S(\omega)| \leq 1$, for $0 < \omega < \omega_p$. Note that it is generally necessary to consider the entire frequency range and not just frequencies below $\omega_{p/2}$ since, no matter how well-controlled S_0 may be, S_{-1} could be such as to yield an unstable product.

The equation for the stability factor, eq. (7), may be solved for Z_x to yield

$$Z_x = -Z_d + \left(\frac{r}{1 + r - S} \right) \left(Z_d - \frac{1}{j\omega C_T} \right), \qquad (11)$$

where

$$r \triangleq \left(\frac{\omega_a^2}{\omega^2} - 1 \right)^{-1}. \tag{12}$$

For any set of Z_d, r, ω, and C_T, eq. (11) may be recognized as a bilinear transformation[7] between Z_x and S. Several properties of a bilinear transformation are useful here:

(i) A chain of bilinear transformations is also a bilinear transformation.

(ii) A bilinear transformation is one-to-one.

(iii) A bilinear transformation always maps circles into circles (the straight line is regarded as a circle of infinite radius).

The third property is particularly useful, since it states that circles of constant $|S|$ map into circles in the external impedance plane. It may be shown that the family of constant $|S|$ circles in the Z_x plane are determined by the graphical construction given in Fig. 8.

It is evident from Fig. 8 that there exists a simply connected region in the Z_x plane such that, for any Z_x within this region, $|S| \leqq 1$. Further, the region is bounded by a circle; in some cases, it may be the entire Z_x plane "outside" a circle. The circle in the Z_x plane for $|S| = 1$ has several important properties. It must pass through the point $Z_x = j(1/\omega C_T)$, as may be readily seen from eq. (7). Also, the circle cannot be tangent to the imaginary axis at $Z_x = j(1/\omega C_T)$, but rather must subtend a portion of the positive-real half of the Z_x plane. The latter property can be seen from Fig. 8, where it is evident that the line of centers cannot be horizontal since, in general, Im $(Z_d) \neq 1/j\omega C_T$. Thus, it is apparent that there is always some region of positive-real Z_x such that $|S| \leqq 1$. Therefore, we can contemplate synthesis of a Z_x function sufficient to give stability using only passive elements.

The boundaries of the stable regions of the Z_x plane have been computed for a specific case, and the results are shown in Fig. 9. By "boundary of the stable region" we mean here the locus of Z_x for which $|S| = 1$. The case considered is that of a diode with Read-model parameters; $C_T = 1$ pF, $\bar{x}_d = 0.83$, $\tau_d = 40$ ps, and $f_a = 7.5$ GHz. These parameters are comparable to the experimental diodes of the previous section, i.e., they are representative of a typical X-band GaAs diode. In Fig. 9, the stable regions are shown for a discrete set of frequencies spanning the range from zero through X-band. The boundaries of the stable regions are circular arcs in the Smith chart, since the transformation from rectangular to Smith chart coordinates is another bilinear transformation.
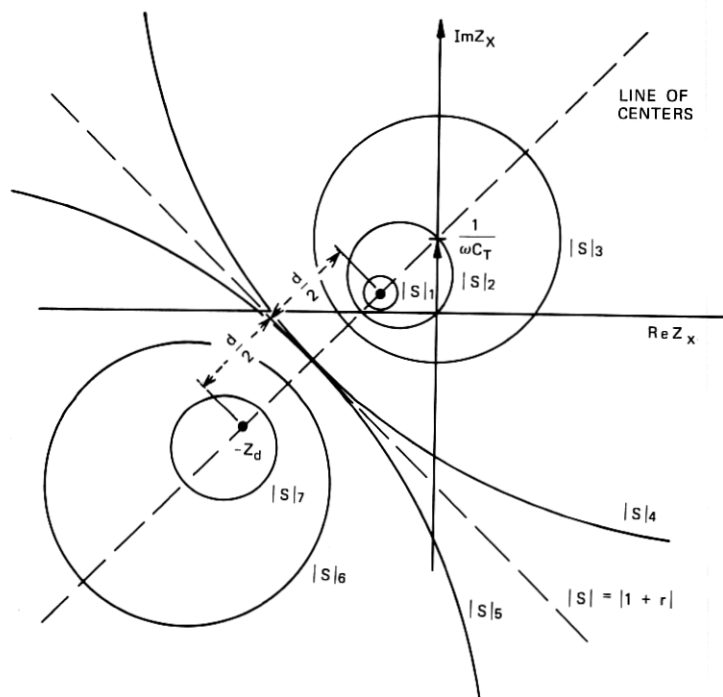
$$|S|_1 < |S|_2 < \cdots \cdots < |S|_7$$

$$\beta = \frac{(1 + r)r}{(1 + r)^2 - |S|^2}$$

$$\gamma = Z_d + j\,\frac{1}{\omega C_T}$$

$$d = \frac{\omega^2}{\omega_a^2}\,|\gamma|$$

$$Z_{CENTER} = -Z_d + \beta\gamma, \quad \text{RADIUS OF Z CIRCLE} = \left|\beta\frac{S}{1 + r}\right||\gamma|$$

Fig. 8—Construction of constant $|S|$ circles in the Z_x plane.

A graph such as Fig. 9 may be used to synthesize a Z_x function to give unconditional stability or to check a proposed Z_x in the following manner. If a proposed $Z_x(\omega)$ is such that at $f = 2$ GHz it falls within the 2-GHz circle, at 4 GHz Z_x lies within the 4-GHz circle, and so on for all frequencies $0 < f < f_p$, then the diode for which Fig. 9 is applicable is unconditionally stable in the circuit corresponding to Z_x. That is, it will not develop parametric-type spurious oscillation for any physically attainable pump level.
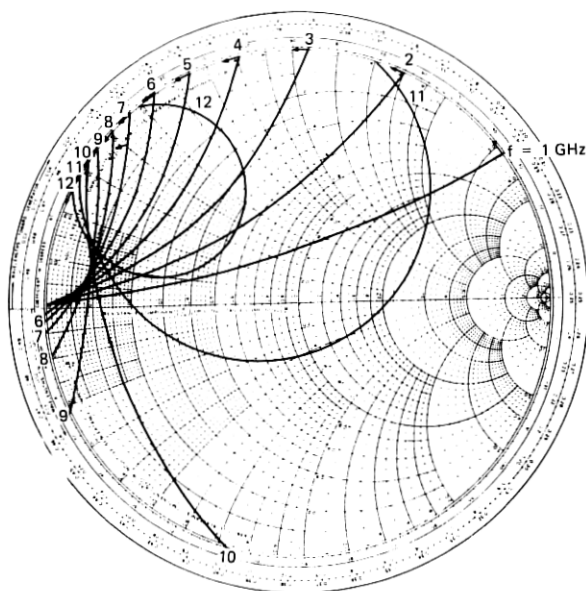
Fig. 9—Stable regions of external impedance for a typical diode. (Arrows indicate stable region. $C_T = 1$ pF, $\bar{x}_d = 0.83$, $\tau_d = 40$ ps, $f_a = 7.5$ GHz, $Z_0 = 50$ ohms.)

The location of the stable regions in Fig. 9 is governed entirely by the four independent parameters of the Read-diode model. Thus, it is of interest to determine the effect of these parameters individually and to construct a more universal diagram. Figure 9 may be interpreted in a more general fashion as follows. Equation (11) may be rewritten as

$$Z_x = \frac{\tau_d}{C_T} \frac{1}{\omega \tau_d} \left[-z + \left(\frac{r}{1 + r - S} \right)(z + j) \right]$$

$$= \frac{\tau_d}{C_T} g(\bar{x}_d, \omega\tau_d, \omega_a\tau_d, S), \tag{13}$$

where

$$z \triangleq \omega C_T Z_d. \tag{14}$$

In eq. (13), the function g depends only upon the parameters $\bar{x}_d$, $\omega_a\tau_d$, S, and the normalized frequency $\omega\tau_d$. Therefore, it is apparent that Fig. 9 may be applied to *any* diode that has $\bar{x}_d = 0.83$ and $\omega_a\tau_d = 0.6\pi$ radians. Of course, the labelled frequencies must be reinterpreted as normalized frequencies, i.e., $f = 2, 4, \cdots, 12$ GHz corresponds to $\omega\tau_d = 0.16\pi, 0.32\pi, \cdots, 0.96\pi$ radians. Also, the

normalizing impedance needs to be reinterpreted as

$$Z_0 C_T / \tau_d = 1.25 \text{ ohm } F \ S^{-1}. \tag{15}$$

Thus, it is evident that the parameters τ_d and C_T affect only scale factor but not the relative size or location of the stable regions in Fig. 9.

Since a chart such as Fig. 9 is applicable to the family of diodes with fixed $\bar{x}_d$ and $\omega_a \tau_d$, it is worthwhile to consider briefly the usual ranges for these parameters that are obtained in practice. The parameter $\bar{x}_d$ is the fraction of the total depletion layer occupied by the drift region. Although this depends in general upon the semiconductor material and doping profile, for a uniformly doped diode $\bar{x}_d$ is essentially constant over a wide range of doping levels.[6] That is, for a GaAs one-sided, uniformly doped, nonpunch-through IMPATT, it is a reasonable approximation to take $\bar{x}_d = 0.83$ for devices that operate within the approximate frequency range 4 to 20 GHz. The transit time τ_d determines the frequency for optimum large-signal operation. In practice, the diode is usually designed so that $\omega_p \tau_d \cong 0.8\pi$. The avalanche frequency depends upon material parameters and also upon the bias current density. However, in practice, it is usually found that $\omega_p/2 < \omega_a < \omega_p$. Thus, the usual range of $\omega_a \tau_d$ is $0.4\pi < \omega_a \tau_d < 0.8\pi$.

Figures 10a and 10b give the stability charts for $\bar{x}_d = 0.83$ and $\omega_a \tau_d = 0.4\pi$ and 0.8π rad. These normalized charts together with Fig. 9 may be used for studying the stability of the most common type of GaAs IMPATT diodes, namely, one-sided, uniformly doped diodes. For other doping profiles or semiconductor material, it is simple to construct similar charts using eq. (13) or the graphical procedure of Fig. 8. It is evident from Fig. 10b that the region of Z_x which gives $|S| < 1$ is quite small at the higher frequencies. This suggests that diodes with large values of $\omega_a \tau_d$ may be quite difficult to stabilize.

Some additional remarks should be made concerning the choice of a Z_x that is sufficient for unconditional stability. One concerns the possibility of compensation at complementary frequencies. Thus far, the discussion has been devoted to finding $Z_x(\omega)$ so that $|S(\omega)| \leqq 1$ for $0 < \omega < \omega_p$. In some practical situations, there may be a portion of this frequency range where it is undesirable or impossible to keep $|S(\omega)| \leqq 1$, perhaps because of the influence of package parasitics. In such a situation, it is still possible to guarantee stability by introducing compensation at the complementary frequency. For example, if for some $\omega_0 |S_0| > 1$, the S-product still lies within the unit disc if $|S_{-1}| < |S_0|^{-1}$. Thus, it may be useful to construct circles in the Z_x plane corresponding to $|S|$ other than unity, to assist in the design of
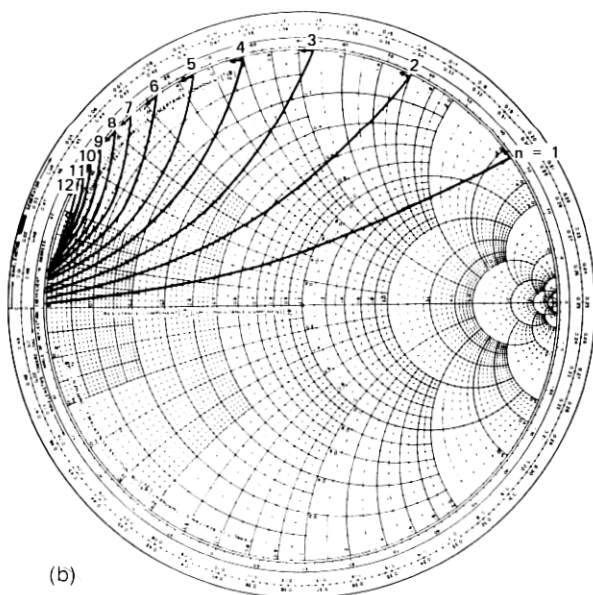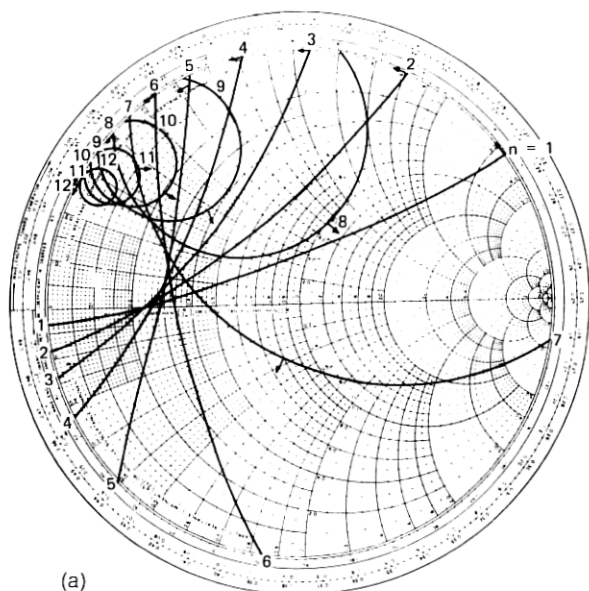
(a)

(b)

Fig. 10—Normalized stability charts for external impedance. (Arrows indicate stable regions. $Z_0 C_T/\tau_d = 1.25$ ohm F S^{-1}.) (a) $\bar{x}_d = 0.83$, $\omega_a\tau_d = 0.4\pi$. (b) $\bar{x}_d = 0.83$, $\omega_a\tau_d = 0.8\pi$.

a compensated Z_x. One drawback to any compensation procedure, however, is that the complementary frequencies are related by ω_p. Therefore, a diode-circuit system that is compensated at ω_{p0}, i.e., that has $S_0 S_{-1}^*$ within the unit circle for ω_{p0}, may be unstable for pump frequencies that are sufficiently different from ω_{p0}.

Furthermore, it is not necessary for unconditional stability that $|S_0 S_{-1}^*| \leq 1$, except at the subharmonic frequency. In applications where this condition is too restrictive of Z_x, it is possible to analyze proposed circuits for stability and study the effect of various circuit parameters. The stability criterion of eq. (10) may be used or, since such an analysis is most conveniently done by computer, the more general expression of eq. (4) may be used with little more cost.

A question arises concerning the compatibility of the impedance requirement resulting from Hines' theory of parametric interaction and the impedance requirements for preventing bias-current oscillation which were recently discussed by Brackett.[2] The origin of the oscillation which Brackett considered is in the dc negative resistance produced in an IMPATT by the large-signal rectification properties of the avalanche process. This is a different physical process from the one Hines considers and, in fact, Hines assumed the induced dc resistance to be zero. Brackett concluded that, to prevent bias-circuit oscillations, the diode should see a high impedance below some cutoff frequency f_c. The value of f_c depends upon the Q of the microwave circuit, but generally f_c is less than about 500 MHz. It may readily be seen from eq. (3) that, for $f < f_c$, the factor $\omega^2/(\omega_a^2 - \omega^2)$ becomes so small that $S \cong 1$ for any finite value of Z_x. Thus, Z_x may be chosen to satisfy Brackett's requirements without appreciably affecting the stability factor.

V. CONCLUSIONS

The aspects of Hines' recent theory of parametric interactions of IMPATT diodes that are most pertinent to the study of stability in strongly driven oscillators and amplifiers have been reviewed. A simple, approximate stability criterion has been developed from Hines' theory. An experiment was performed in which several cases of spurious oscillation were observed, and the diode and circuit impedances were carefully characterized for each case. The predictions of the stability criterion were found to be in good quantitative agreement with the experimental observations in each case.

Using the simple stability criterion, a procedure has been developed for determining a range of circuit impedance sufficient for unconditional stability, i.e., stability under all physically attainable drive

levels. The desired circuit impedance is expressed in terms of the Read-model equivalent of the IMPATT diode in question. A set of normalized stability charts has been given that may be used for designing stable circuits for a class of GaAs IMPATT diodes. The procedure is also given for constructing similar charts for other types of diodes.

The desired circuit behavior appears to be synthesizable using positive-real impedance functions. Finally, it has been shown that the circuit requirements are compatible with the restrictions described by Brackett to prevent bias-circuit oscillations and low-current burnout.

VI. ACKNOWLEDGMENTS

APPENDIX

This appendix compares the values of modulation index M_1 which were measured at the threshold of spurious oscillation to those predicted by the stability criterion, for the cases discussed in Section III. The measured values of M_1 are calculated as follows:

$$|M_1| \triangleq \frac{|I_o|}{2I_{dc}},$$

where

$$I_o = (1 - \bar{x}_d - j\beta\bar{x}_d)^{-1}I_e,$$
$$\beta = (1 - e^{-j\omega_p\tau_d})/\omega_p\tau_d,$$
$$I_e = I_T(Y_d - j\omega_p C_T)/Y_d,$$
$$|I_T| = (2P/R_x)^{\frac{1}{2}},$$
$$Y_d = (-Z_x)^{-1},$$

and

I_o = injected current (*full* wave amplitude),

I_e = induced current,

I_T = terminal current,

Y_d = diode large-signal admittance at the pump frequency,

P = output power at the pump frequency,

R_x = Re (Z_x).

Table III — Modulation index M_1 at threshold of spurious oscillation

	Measured	Theoretical
Case 1	0.49	0.61
Case 2	0.69	0.68
Case 3	0.58	0.69

The magnitude of the modulation index was evaluated using the data given in Section III. The results are compared to the theoretical spurious threshold in Table III. The agreement is considered to be reasonably good, when the approximations of the stability criterion and the diode model are considered.

REFERENCES

1. M. E. Hines, "Large-Signal Noise, Frequency-Conversion and Parametric Instabilities in IMPATT Diode Networks," Proc. IEEE, *60*, No. 12 (December 1972), pp. 1534–1548.
2. C. A. Brackett, "The Elimination of Tuning-Induced Burnout and Bias Circuit Oscillations in IMPATT Oscillators," B.S.T.J., *52*, No. 3 (March 1973), pp. 271–306.
3. W. T. Read, Jr., "A Proposed High-Frequency Negative Resistance Diode," B.S.T.J., *37*, No. 2 (March 1958), pp. 401–446.
4. M. Gilden and M. E. Hines, "Electronic Tuning Effects in the Read Avalanche Diode," IEEE Trans., *ED-13* (January 1966), pp. 169–174.
5. C. N. Dunn and J. E. Dalley, "Computer-Aided Small-Signal Characterization of IMPATT Diodes," IEEE Trans. MTT, *17*, No. 9 (September 1969), pp. 691–695.
6. W. E. Schroeder and G. I. Haddad, "Nonlinear Properties of IMPATT Devices," Proc. IEEE, *61*, No. 2 (February 1973), pp. 153–182.
7. R. V. Churchill, *Complex Variables and Applications*, 2nd ed., New York: McGraw-Hill, 1960, pp. 73–80.